International Journal of Civil and Structural Engineering Research ISSN 2348-7607 (Online)
Vol. 5, Issue 2, pp: (53-62), Month: October 2017 - March 2018, Available at: www.researchpublish.com

DEVELOPING LOAD TRANSFER MODELS FOR DRILLED SHAFTS

[1]Thuy Vu, [2]Erik Loehr, [3]Douglas Smith

[1]Department of Civil Engineering, University of Texas Rio Grande Valley, 1201 W. University Dr., Edinburg, TX, 78539. *E-mail: thuy.vu@utrgv.edu*

[2]Department of Civil Engineering, University of Missouri Columbia, 105 Jesse Hall, Columbia, MO, 65211. *E-mail: eloehr@missouri.edu*

[3]Department of Mechanical Engineering, Baylor University, Waco, Texas 76798, *E-mail:Douglas_E_Smith@baylor.edu*

Abstract: **This paper presents the development of load transfer models and their variability values for use in probabilistic analysis and design of drilled shafts at service limit state. The development used intensive regression analysis on full scale load test data. The analyses were carried out for both side resistance and tip resistance. Five functional models, and two different types of regression analyses were performed, non-weighted least squares regression and weighted least squares regression. The hyperbolic function obtained from non-weighted least squares regression was found to fit the load transfer data best. This paper also presents the effects that the two load transfer normalization approaches have on the resistance factors: the normalization-to-maximum measured values approach and normalization-to-maximum predicted approach. The recommendation is when developing load transfer *t-z* curves, the normalization-to-maximum measured values approach is preferred to use.**

Keywords: **Load and resistance factor design (LRFD); Regression analysis; Foundation design; Resistance factors; Service limit state; Probabilistic analyses.**

1. INTRODUCTION

Geotechnical engineers are moving from allowable stress design to load and resistance factor design (LRFD). Allowable stress design is the traditional design method, and its safety margin has gained widespread acceptance within the engineering community. The factor of safety for each type of structure is chosen based on past experience. However, design engineers seldom explicitly know the reliability of their designs or the probability of failure. On the other hand, LRFD is often linked explicitly to reliability analysis, and load factors and resistance factors are used to account for sources of variability and uncertainty in design. An LRFD design often is targeted at a known level of reliability P_f. The LRFD approach, therefore, provides the potential to achieve more consistent and uniform reliability. The American Association of State Highway and Transportation Officials (AASHTO) has made utilization of LRFD mandatory on all federally-funded new bridge projects (AASHTO, 2012). Research has focused on the issue of SLS design using LRFD methods (Misra & Roberts, 2009, Wang et al., 2011, Reddy and Stuedlein 2017, Vu and Loehr 2015, 2017). Vu and Loehr (2017) proposed a design procedure that utilizes strength resistance factors calibrated for a design to achieve a target probability of failure. The procedure can be used for varying values of the target probability of failure, and allows the shaft dimensions, soil strength, variability of soil strength, loads, and allowable settlement to be adjusted freely in the design. The procedure eliminates the need to establish resistance factors for the SLS on a case-by-case basis, which is a current practical issue for LRFD. The procedure utilizes the *t-z* analyses and adopts the "factored strength" approach to LRFD (Becker, 1996; Salgado, 2008), which is different from the factored resistance approach currently used in AASHTO design provisions. The resistance factors apply to soil strength parameters to account for variability and uncertainty in the design method and associated input parameters. The primary appeal of the proposed procedure is that it eliminates the need to design for the SLS for case specifics, while still being practical enough for routine implementation, and has the advantage of producing a foundation that achieves a target probability of exceeding a selected target value of settlement. This represents an improvement over historical allowable stress design practice and represents the crux of LRFD methods. The procedure for design of drilled shafts in shale at the SLS can be summarized in the following five steps:

Step 1: Determine the initial shaft dimensions using strength limit state criteria and calculate the nominal shaft capacity.

Step 2: Compute the shaft length-to-diameter ratio *L/D*, and normalized load, θ, as the ratio of factored load and nominal shaft capacity.

Step 3: Calculate the resistance factor, φ, as a function of θ, *L/D*, target probability of failure P_f, and coefficient of variation (COV) of the uniaxial compressive strength (UCS).

Step 4: Using factored uniaxial compressive strength determine the factored shaft head's vertical displacement, y^*, using appropriate t-z analyses software.

Step 5: Check whether the design requirement is satisfied by comparing y^* to the established allowable settlement, y_a. Repeat Steps 1 through 5 for progressively larger drilled shafts until the condition of $y^* \le y_a$ is satisfied.

2. LOAD TRANSFER (*T-Z*) METHOD AND LOAD TRANSFER MODELS

The load transfer or *t-z* method is one of the more rigorous methods used to determine the vertical shaft head displacement (Brown et al. 2010, O'Neil and Reese 1999, Misra and Roberts 2009). Solving for shaft settlement usually requires iterations and a computer program is often needed. Figure 1 shows the shaft sectioned or divided into a number of elements. Application of the *t-z* method requires *predictive models* to predict the ultimate unit resistance (side and tip) and *load transfer models* to predict mobilized resistance. Predictive models are used to establish ultimate side and tip resistances from geomaterial properties, in this case the property is uniaxial compressive strength. Load transfer models are used to predict mobilization of resistance along the shaft and tip of the shaft: a load transfer curve for side resistance or "*t-z* curve" represents the relationship of a normalized unit side resistance versus displacement at the shaft-soil interface; a load transfer curve for the tip resistance or "*q-w* curve" is the relationship of a normalized unit tip resistance versus tip displacement (Figure 1). Mobilized unit resistance is determined using two steps:

- Step 1, *Mobilization*: Obtain the mobilized normalized unit resistance associated with a normalized displacement using load transfer curves.
- Step 2, *Prediction:* Multiply the mobilized normalized unit resistance obtained from Step 1 with a predicted ultimate unit resistance.

Ultimate unit resistance and load transfer models are usually developed from full-scale load test data. For this research, ultimate unit resistance models were developed from the load test measurements for full-scale drilled shafts founded in shale (Loehr et al., 2011). The load tests were predominantly performed in Missouri, but also included tests performed in Kansas, Colorado, Iowa, and Kentucky. Both models are taken to be functions of uniaxial compressive strength, (UCS):

$$q_s = 1.71 \times UCS^{0.79} \le 1{,}436 \text{ kPa} \qquad (3)$$

$$q_t = 43.0 \times UCS^{0.71} \le 19152 \text{ kPa} \qquad (4)$$

where q_s is the ultimate unit side resistance and q_t is the ultimate unit tip resistance. The variability and uncertainty associated with these models were quantified by a coefficient of variation of 0.66 and 0.25, respectively.

Load transfer models are developed using data from full scale load tests, this research used load test data on drilled shafts founded in Missouri shales (Vu, 2013). The load transfer models are in the normalized form, and when developing the models from load test data, there are two different approaches of normalization: 1) normalizing the mobilized unit resistance using the maximum *measured* values of the unit resistance and 2) normalizing the mobilized unit resistance using the maximum *predicted* values. The first approach presumes that the maximum measured resistance represents the ultimate condition, which may or may not be appropriate for specific data. The latter approach, in contrast, presumes that a reasonable prediction method exists for the materials present, and mobilized side and tip resistance values for each shaft segment were normalized using predicted values of ultimate unit resistance.These predicted values used for normalization were established using Equations 3–4. Both of these approaches were utilized for the load test measurements to develop load transfer models.

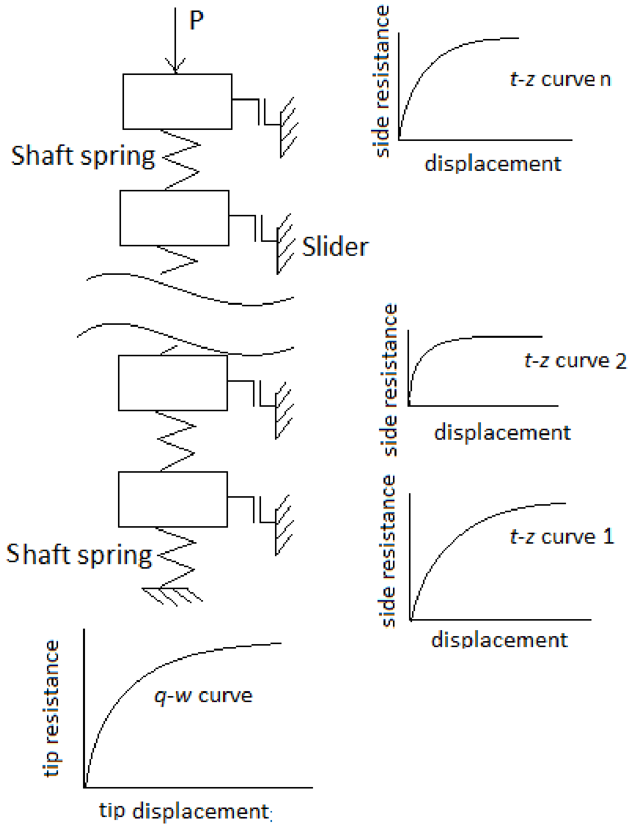

Figure 1: Load transfer model and load transfer curves.

For the approach of normalizing to maximum measured resistance, the *t-z* models obtained from the approach have a maximum *y* axis value of 1.0 as in Figure 2, and the curve only carries the load transfer variability/uncertainty. Thus, the variability of the results in Step 1 comes only from the variability of load transfer; and that of Step 2 comes from the variability of the prediction model (Equations 3 & 4). Meanwhile, for the approach of normalizing to the predicted ultimate resistance, the load transfer curve can have any *y* axis value (but not maximum of 1.0, as when the load transfer is normalized to the maximum measured resistance) as shown in Figure 2(b). A load transfer model thus carries both the load transfer model's uncertainty (mobilization - Step 1) and the prediction model's uncertainty (prediction – Step 2). The reason is that the *t-z* models used here were obtained by normalizing unit resistance with the predicted ultimate unit resistance, so the uncertainty of the ultimate unit resistance prediction is inherently within the models. This explains why the variability of the result in Step 1 comes from both the variability of load transfer models and prediction models. Therefore, during the analysis, the variability in Step 2 was set to zero to avoid redundancy. Resistance factors obtained from the two different approaches will be calculated and compared to make recommendations.

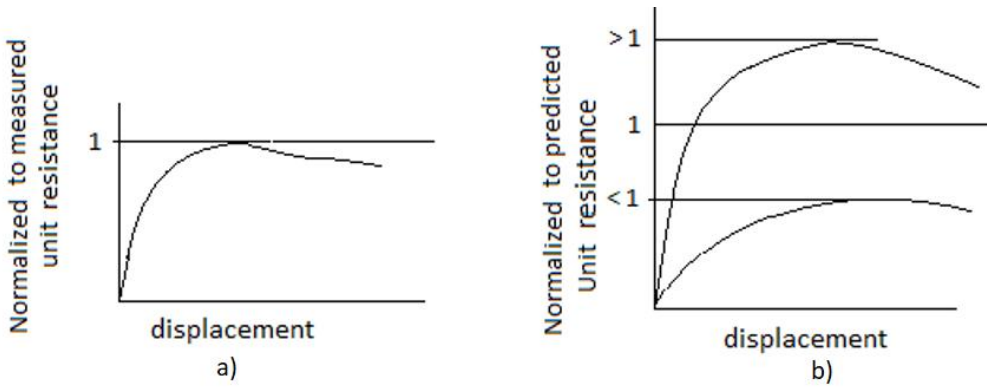

Figure 2: The *t-z* curves for a) normalized to maximum measured unit resistance and b) normalized to maximum predicted unit resistance.

3. REGRESSION ANALYSIS: NON-WEIGHTED LEAST SQUARES REGRESSION VERSUS WEIGHTED LEAST SQUARES REGRESSION

Load test data will be analyzed using two different types of regression analyses: *non-weighted least squares (NLS)* regression and *weighted least squares* (WLS) regression. Figure 3 illustrates the differences between these two regression analysis procedures. The non-weighted least squares regression is based on the assumption that the data exhibit constant variance (or constant conditional standard deviation) about the trend line (Ang and Tang, 2004). The constant standard deviation, $\sigma_{y/x}$, over the range of data is shown in Figure 3(a) by the parallel bounds. The assumption of constant variance is commonly exhibited in many data sets. In non-weighted least squares regression, parameter estimates for the selected regression functions are found by minimizing the sum of the squared residuals between the data points and the prediction model. Some data sets however may not exhibit constant standard deviation about the trend line as in Figure 3(a), but rather may exhibit standard deviation that depends on the value of the predictor variable, as illustrated in Figure 3(b). In such cases, weighted least squares regression is preferable

to ensure that each data point has an appropriate influence on the final parameter estimates. In weighted least squares regression, the *weighted* sum of the squared residuals between the data points and the prediction model is minimized to determine the parameter estimates. A variety of different weights can be used in weighted least squares regression, with the weights dictating the values of the parameter estimates as well as how the conditional standard deviation varies with the magnitude of the predictor variable. This study used regression weights that were chosen to be inversely proportional to the magnitudes of the predictions, i.e., to be equal to $1/y$, where y is the value of the prediction for a given x (Ang and Tang, 2004). Using such weights produces the convenient result of having a constant coefficient of variation (standard deviation divided by the mean), and sometimes can offer a good representation of the scatter around the regression line for many data sets.

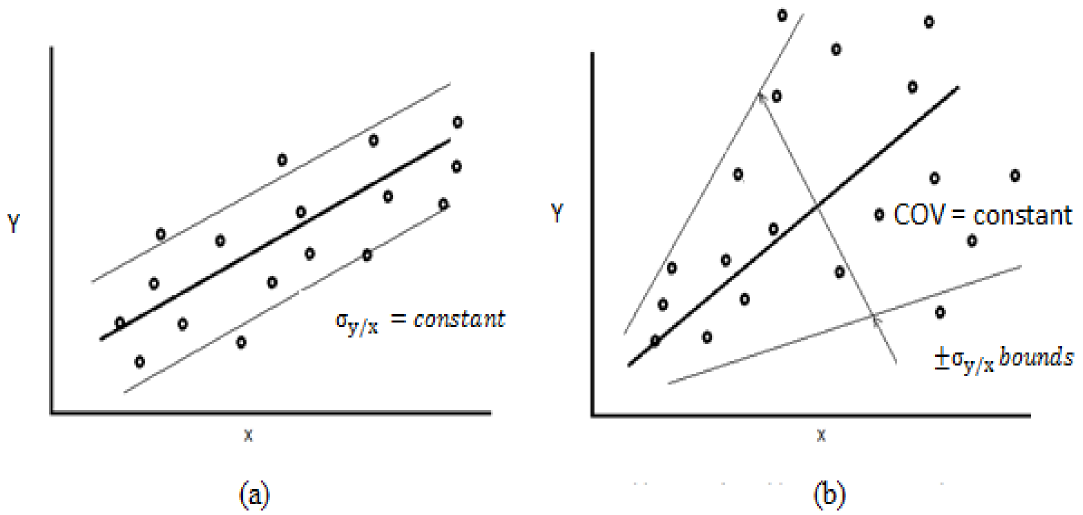

Figure 3: Illustration of regression under: (a) constant standard deviation and (b) no-constant standard deviation (after Ang and Tang, 2004).

4. MODELING OF LOAD TRANSFER *T-Z* CURVES

Normalized unit resistance data were fit to find load transfer models using five different functional forms. Table 1 lists each form as a nonlinear combination of model parameters and normalized axial displacement (as percentage of shaft diameter %D). These functional forms include power, exponential, logarithm, rational and hyperbolic function fitting. Both non-weighted and weighted least squares regression analyses were performed for each of the five functional forms. Standard and customized MATLAB® functions were used to find the model that best reflects the load transfer data and their variability/uncertainty. Important criteria used for choosing the best model is based on the root-mean-square error ($RMSE$). Table 1 presents the models for each function, where t and q are the normalized unit side and tip resistance, normalized to *maximum measured* values, and z and w are the normalized displacement of the local shear zone. The *RMSE*s and summary of advantages and disadvantages of each function are also included. NLS and WLS analyses produced different functional models as well as different quantified variability of the data.

International Journal of Civil and Structural Engineering Research ISSN 2348-7607 (Online)
Vol. 5, Issue 2, pp: (53-62), Month: October 2017 - March 2018, Available at: www.researchpublish.com

a. Side load transfer (t-z) model:

For power function, the model trends and the $\pm\sigma_{y|x}$ bounds (68.2% confidence bounds for new observations) are imposed with the field test data as shown in Figure 4. The model trends fit the data well at normalized displacements of less than about 4% (NLS) and 2% (WLS). However, the model trends overestimate the mobilized unit side resistance at greater normalized displacements, which exposes the major disadvantages of the function. This overestimation increases without a bound and is problematic. Also, the initial slope of the power function is infinite, which may pose numerical problems in modeling load transfer.

Note how the $\pm\sigma_{y|x}$ bounds from NLS regression analyses are "parallel" to the model trend, and the vertical distance from a bound to the model trend is constant and equal to the model's *RMSE*. In contrast, the bounds from WLS regression deviate from the model trend starting from the point of origin, showing a constant COV. WLS analysis generates a higher *RMSE* of 0.50 compared to that from NLS of 0.20.

Table 1: Side and tip load transfer model fitting

Functions and Regression Type	Equations for side resistance	*RMSE* side resistance	Equations for tip resistance	*RMSE* tip resistance	Advantages/ disadvantages
Power NLS	$t = 0.75\ z^{0.22}$	0.20	$q = 0.48w^{0.34}$	0.13	Overestimate data when displacement is large; infinity slope at origin; high *RMSE*.
Power WLS	$t = \ 0.84\ z^{0.34}$	0.50	$q = 0.48w^{0.39}$	0.40	
Exponential NLS	$t = 1 - \ \exp(-4.06z)$	0.19	$q = 1 - exp(-0.78w)$	0.16	Fit data well when displacement is large; trace the upper bound well, but high *RMSE*.
Exponential WLS	$t = 1 - \ \exp(-9.67z)$	1.41	$q = 1 - exp(-2.55\ w)$	0.82	
Logarithm NLS	$t = 0.15\ \ln(z)\ + 0.79$	0.19	$q = \ 0.13\ \ln(w)\ + 0.52$	0.15	Overpredict side resistance data and underpredict tip resistance, relatively high *RMSE*.
Logarithm WLS	$t = 0.09\ln(z)\ + 0.67$	0.48	$q = 0.08ln(w) + 0.44$	0.46	
Rational NLS	$t = \dfrac{0.95z + 0.007}{z + 0.14}$	0.17	$q = \dfrac{1.05w + 0.16}{w + 1.36}$	0.13	Model trends do not pass through origin.
Rational WLS	$t = \dfrac{1.01z + 0.02}{z + 0.21}$	0.49	$q = \dfrac{0.90w + 0.07}{w + 0.80}$	0.41	
Hyperbolic NLS	$t = \dfrac{z}{1.07z + 0.13}$	0.17	$q = \dfrac{w}{1.1w + 0.72}$	0.14	Well reflect data and their variability.
Hyperbolic WLS	$t = \dfrac{z}{1.07z + 0.13}$	0.62	$q = \dfrac{w}{1.12w + 0.69}$	0.76	

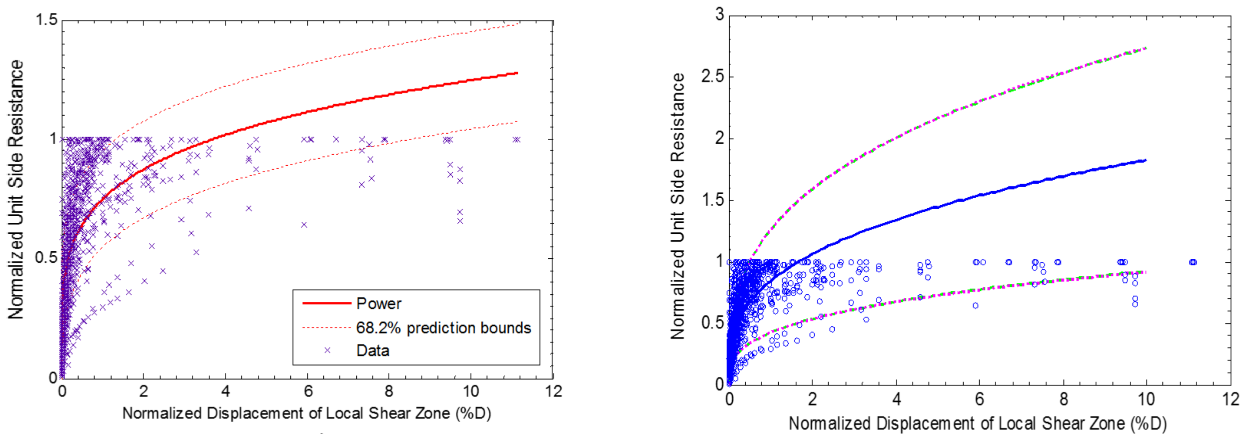

a. NLS regression.   b. WLS regression.

Figure 4: Power function fitting: normalized unit resistance vs. normalized displacements

For exponential function, the model trends track the load transfer data well when the displacement is less than 2% D where most of the data points are clustered as shown in Figure 5; then, the trends do not fit the data well. Moreover, the bounds obtained from WLS analysis appear unreasonable with the lower bound passing to a value of −0.5. Instead of the bounds encompassing 68% of the data points, the bounds seem to cover 100% of the data points, which should not be the case.

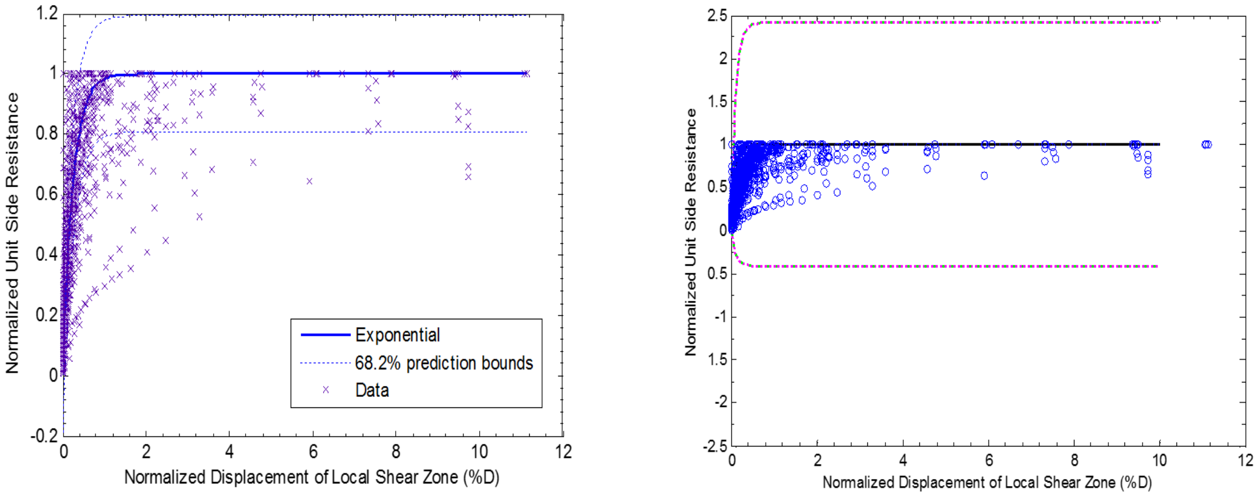

a. NLS regression. b. WLS regression

Figure 5: Exponential function fitting: normalized unit resistance vs. normalized displacements

For logarithm function, the model trend from NLS regression reflects the data well when the normalized displacement is small as shown in Figure 6,; however, the model overpredicts future outcomes at greater displacements, i.e., when the displacement exceeds 4% of the shaft diameter. The WLS model trend better reflects the observed load transfer data, where the model lies in the center of the of the data cluster for the whole range of displacements. However, the WLS analysis produces a high *RMSE* of 0.48 (compared to an *RMSE* of 0.19 from NLS analysis), and WLS $\pm\sigma_{y|x}$ bounds encompass most data and overpredict the variability of future outcomes.

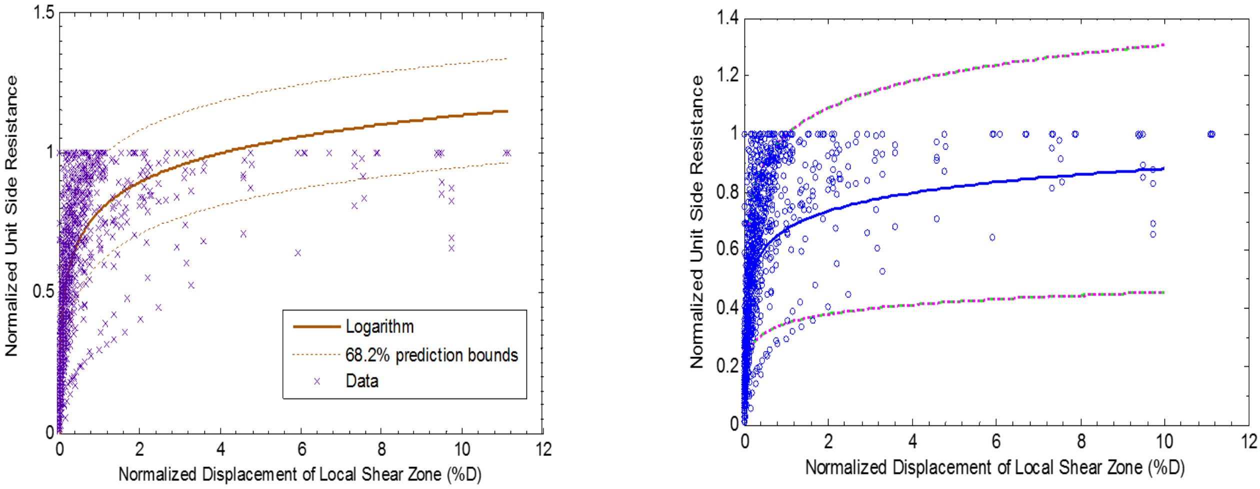

a. NLS regression. b. WLS regression.

Figure 6: Logarithm function fitting: normalized unit resistance vs. normalized displacements

For rational function, the model trends follow the data pattern well as shown in Figure 7. The *RMSE* from the NLS is 0.17, which is the lowest so far. The bounds from WLS regression overestimate the variability of future outcomes when the bounds cover up approximately 90% of the data, which is more than 68%. However, the NLS and WLS rational model trends do not pass through the origin, and there is a non-zero response at zero displacement.

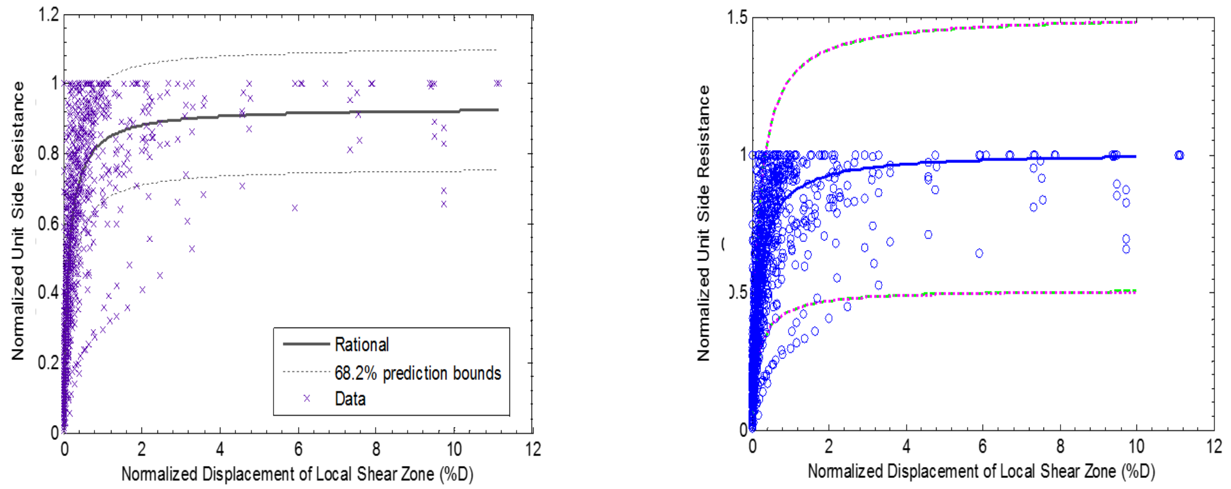

a. NLS regression. b. WLS regression.

Figure 7: Rational function fitting: normalized unit resistance vs. normalized displacements.

For hyperbolic function, the NLS and WLS regression analyses gave the model trends that reflect the data well as shown in Figure 8, and produced the same hyperbolic equations (when two significant numbers are considered for the fitting parameters). The bounds from the NLS analysis reflect the scatter of the data well with the lowest *RMSE* of 0.17 (which matches the *RMSE* from NLS analysis using a rational model). The bounds from WLS, in contrast, cover more than 90% of the data points, and the *RMSE* is significantly larger.

Out of the five functional models, the hyperbolic model from the NLS analysis best fits the load transfer data for individual drilled shafts in shales, and the hyperbolic model with NLS regression best reflects the side resistance data and their variability and uncertainty.

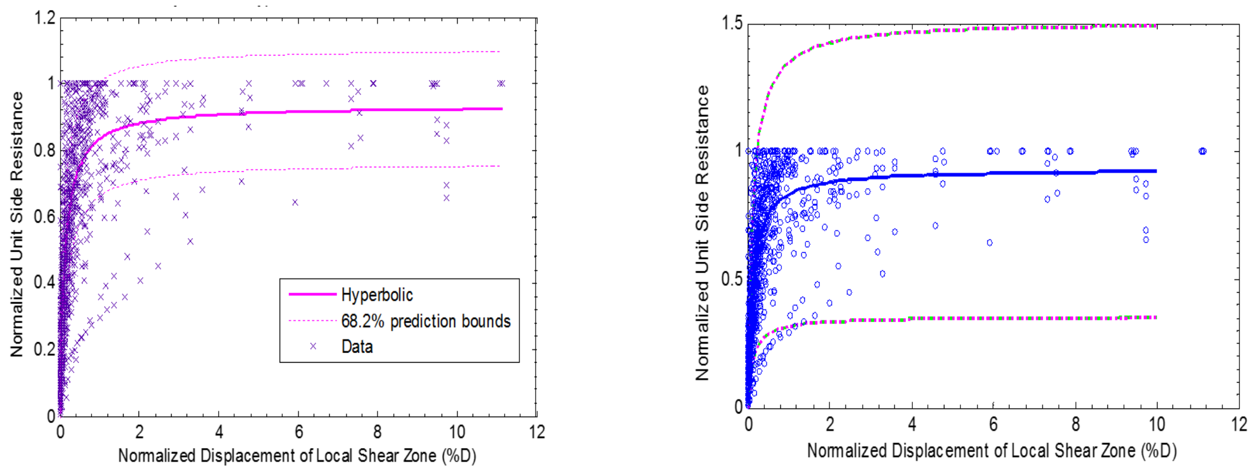

a. NLS regression. b. WLS regression.

Figure 8: Hyperbolic function fitting: normalized unit resistance vs. normalized displacements.

b. Tip load transfer (q-w) model:

General observations for tip load transfer modeling are similar to the information gathered for side (Vu, 2013). The prediction bounds from the NLS are better than those from WLS regression for the most part. WLS can only better predict the variability of the data when the displacement is relatively small, usually less than 0.05% D; when the displacement is larger, the bounds overpredict the future data variability. NLS regression gave *RMSE* values that were significantly smaller than those from the WLS regression analyses; thus, NLS regression is recommended for the analyses.

Five model trends from the NLS regression analyses and the field test data on the normalized unit side and tip resistance are shown in Figure 9. To summarize, the power function underestimates future data when the displacement is small (2% D) and overestimates future data when the displacement is larger than 4% D. The exponential model trend best reflects

International Journal of Civil and Structural Engineering Research ISSN 2348-7607 (Online)
Vol. 5, Issue 2, pp: (53-62), Month: October 2017 - March 2018, Available at: www.researchpublish.com

the observed data when the displacement is 1% up to 4% D, and then follows the upper bound of the data when the displacement is larger. The logarithm overpredicts side resistance data and underpredicts tip resistance data. The rational and hyperbolic models have model trends that reflect the data well, and the model trends from the two functions are close together. A subtle difference between the two functions is that the trend from the rational model does not pass through origin. As in the case of side load transfer model, the hyperbolic model best reflects data and their variability for the tip load transfer model. The hyperbolic model does not contain practical issues such as an infinite slope at the origin as does the power function, nor does it have a non-zero response at zero displacement as does the rational function. Hyperbolic models also give the lowest *RMSE*s and narrow $\pm\sigma_{y|x}$ prediction bounds. Finally, side and tip load transfer models obtained from NLS analysis on the load test data in the hyperbolic functional forms are:

$$t = \frac{z}{az+b} = \frac{z}{1.07*z+0.13} \quad (5)$$

$$q = \frac{w}{aw+b} = \frac{w}{1.1*w+0.72} \quad (6)$$

The variability of the collective models is reflected by the conditional SD of the fitting model, 0.17 for side and 0.14 for tip resistance. Note that the normalized resistance ranging from 0.0 to 1.0, these values give an intuitive picture of the range of variability in data.

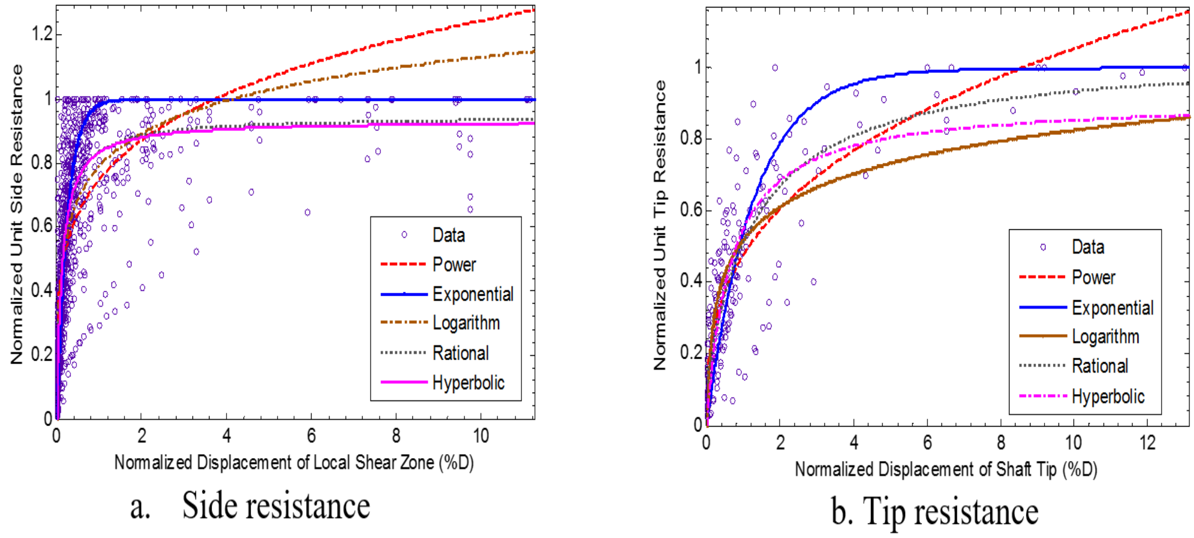

Figure 9: Results of five functional models from NLS regression

5. LOAD TRANSFER NORMALIZED TO PREDICTED ULTIMATE VALUES VERSUS NORMALIZED TO MEASURED ULTIMATE VALUES

The regression analysis presented (Section 4) was for load transfer models development for normalized unit resistance that was normalized by maximum measured values. The hyperbolic functional model and NLS regression analysis were found to be the best approach to obtain the load transfer model. Thus, hyperbolic functional model and NLS regression analysis were used to analyze the normalized unit resistance that was normalized to *maximum predicted* values. The load transfer models for side and tip resistance are expressed as:

$$t = \frac{z}{1.10*z+0.12} \quad (7)$$

$$q = \frac{w}{0.72*w+0.68} \ . \quad (8)$$

The variability/uncertainty of the models is represented by the standard deviation; for the *t-z* model (Equation 7), the standard deviation is 0.35, and for the *q-w* model (Equation 8) it is 0.34. The variability/uncertainty in the two steps of mobilization and prediction were incorporated for resistance factors calibration. Since there two approaches of normalizing load transfer data are different with different uncertainty/variability, the calibrated resistance factors must be different. Figure 10 compares the resistance factors calibrated using load transfers from the two approaches of normalizing. The resistance factors were calibrated for three sample cases (A, B and C) pertaining to different given probabilities of failure and normalized loads. In Case A , P_f = 1/25, and Θ = 0.3. In Case B, P_f = 1/50, and Θ = 0.25. In Case C, P_f = 1/100, and Θ = 0.2. Notably, the resistance factors obtained from the approach of normalizing to predicted ultimate values (solid lines) are consistently lower than the resistance factors obtained from the approach of normalizing to the maximum measured values (dashed lines). The differences come from the incorporation of the uncertainty/ variability of the load transfer models and predictive models as discussed (Section 2). The approach of normalizing to maximum measured resistance produces higher resistance factors, making the design more cost-effective as it achieves the same target probability of failure, and the approach is recommended for use.

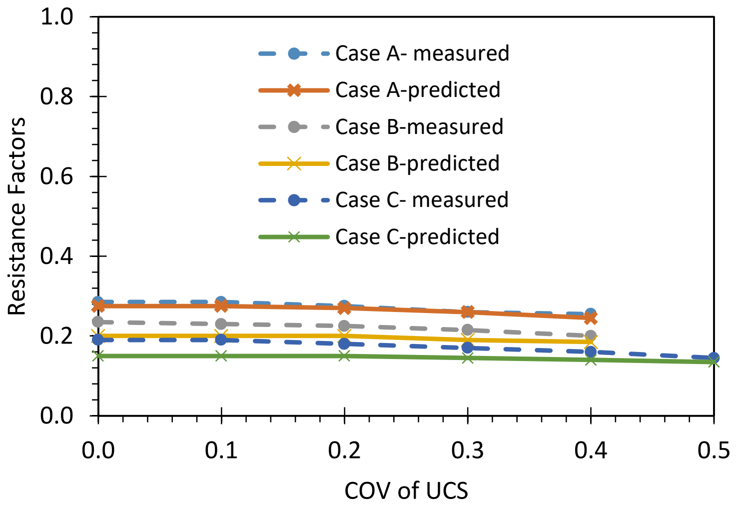

Figure 10: Resistance factors for two approaches of normalization.

6. CONCLUSIONS

Non-weighted least square and weighted least square regression analyses were performed to obtain side and tip load transfer models. Five functional models include power, exponential, logarithm, rational and hyperbolic were tried out to find the best to model the data and to find load transfer models for drilled shafts in shales. This study provides three recommendations: 1) Out of functional models considered, the best model is the hyperbolic model, which successfully predicts future measurements for side and tip load transfer and their variability; 2) non-weighted least squares regression produces better prediction bounds of future observations than weighted least squares regression does. 3) Normalizing by maximum measured values is recommended for analyzing load transfer data for individual drilled shafts in shales.

REFERENCES

[1] AASHTO, LRFD Bridge Design Specifications. 2012. *American Association of State Highway and Transportation Officials, Washington, DC*.

[2] Ang, A. H. S., & Tang, W. H. (2004). Probability concepts in engineering. *Planning*, *1*(4), 1.3-5.

[3] Becker, D. E. (1996). Eighteenth Canadian Geotechnical Colloquium: Limit states design for foundations. Part I. An overview of the foundation design process. *Canadian Geotechnical Journal*, *33*(6), 956-983.

[4] Brown, D. A., Turner, J. P., & Castelli, R. J. (2010). *Drilled shafts: Construction procedures and LRFD design methods*: US Department of Transportation, Federal Highway Administration.

[5] Loehr, J. E., Bowders, J. J., Ge, L., Likos, W.J., Luna, R., Maerz, N., Stephenson, R.W. (2011). Engineering Policy Guidelines for Design of Drilled Shafts. No. NUTC R243-2/R244-2

[6] Misra, A., & Roberts, L. A. (2009). Service limit state resistance factors for drilled shafts. Geotechnique, 59(Compendex), 53-61.

[7] O'Neil, M. W., & Reese, L. C. (1999). Drilled shafts: Construction procedures and design methods. TRB Report, 794 p.

[8] Reddy SC, Stuedlein AW. (2017*)*. Serviceability limit state reliability-based design of augered cast-in-place piles in granular soils. Canadian Geotechnical Journal 54.

[9] Salgado, R. (2008), *The Engineering of Foundations*, McGraw-Hill, 882 pp

[10] Vu, T. (2013). "Load and resistance factor design of drilled shafts at the service limit state." PhD dissertation, University of Missouri-Columbia.

[11] Vu, T., Loehr, E. (2015) *Service Limit State Design for Individual Drilled Shafts in Shale Using t-z Method*. IFCEE 2015: pp. 227-236.

[12] Vu, T., Loehr, E. (2017) *Service Limit State Design for Individual Drilled Shafts in Shales.* Journal of Geotechnical and Geoenvironmental Engineering143(12)

[13] Wang, Y., Au, S. K., & Kulhawy, F. H. (2011). "Expanded Reliability-Based Design Approach for Drilled Shafts." *Journal of Geotechnical and Geoenvironmental Engineering,* 137, 140.